

# Tunable Thermoelectric Superconducting Heat Pipe and Diode

F. Antola,<sup>1</sup> A. Braggio,<sup>1</sup> G. De Simoni,<sup>1</sup> and F. Giazotto<sup>1</sup>  
 NEST Istituto Nanoscienze-CNR and Scuola Normale Superiore, I-56127 Pisa, Italy

(\*Electronic mail: [filippo.antola@sns.it](mailto:filippo.antola@sns.it))

Efficient heat management at cryogenic temperatures is crucial for superconducting quantum technologies. In this study, we demonstrate the heat diode performance of a gap asymmetric superconducting tunnel junction. Our results show that the mechanism of bipolar thermoelectricity, which occurs when the hot side has the larger gap, boosts heat rectification. This improvement is consistent for a broad range of thermal biases and for different values of the superconducting gaps. Additionally, we demonstrate that bipolar thermoelectricity can act as a heat pipe, reducing heat losses towards cold terminals and increasing overall efficiency up to 65%. Finally, we show that by adjusting the electrical load, it is possible to tune the heat pipe and diode performances.

Nanoscale thermal transport management<sup>1–6</sup> has become a focal point of interest for its quantum technology applications in cooling<sup>7,8</sup>, energy harvesting<sup>9–12</sup>, and radiation detection<sup>13,14</sup>. A key breakthrough is the heat diode, which enables autonomous directional thermal flow control by making the heat current non-reciprocal concerning the direction of the applied temperature gradient<sup>15–23</sup>. Achievements in the rectification of electronic heat currents have been noted in various tunneling junctions, including those between normal metals and superconductors or Josephson junctions, where non-linear temperature dependencies of the state density significantly enhance rectification efficiencies<sup>24,25</sup>.

In this letter, we demonstrate how the bipolar thermoelectric properties of an SIS' junction<sup>26–30</sup>, where "I" stands for an insulating barrier, and "S" and "S'" represent two different superconducting electrodes, have the potential also to significantly enhance the system's heat rectification across various thermal biases and superconducting gap values. Moreover, in the bipolar thermoelectric regime, we exploit an interesting approach to power management that, by transforming part of the produced energy into Joule heating dissipated on a remote load resistor, effectively implements an electronic heat pipe. This process enables not only to optimize the heat management of the device, but also allows for an electronic control over heat fluxes, which is crucial for the efficiency of cryogenic temperature systems.

To evaluate the performance of our system, we investigate the thermal and electrical behaviors of a superconducting junction as the one in Fig. 1(a), with two superconductors  $S_\alpha$  ( $\alpha = R, L$ ), characterized by their respective electronic temperatures,  $T_\alpha$ , and their energy gaps,  $\Delta_\alpha(T_\alpha)$ . Our analysis exclusively targets the quasiparticle transport, which can be isolated from the Josephson contribution through a specific junction design or by applying a magnetic field<sup>27,31,32</sup>. However, a moderate Josephson effect does not entirely suppress this phenomenon, as reported in Ref. 33 and 34, promising a phase coherent control to the heat performances of the device.

In our model, we assume the electronic distribution of each electrode to be in equilibrium, following the Fermi-Dirac distribution for quasiparticles  $f_\alpha(E_\alpha, T_\alpha) = (1 + e^{E_\alpha/k_B T_\alpha})^{-1}$ , with  $E_\alpha = E - \mu_\alpha$ . To calculate the IV characteristics of the device, we apply a potential difference  $\mu_L - \mu_R = -eV$  across the junction, *i. e.* we adopt a so-called active driving circuitual configuration, illustrated in the left side of Fig. 1(a). In

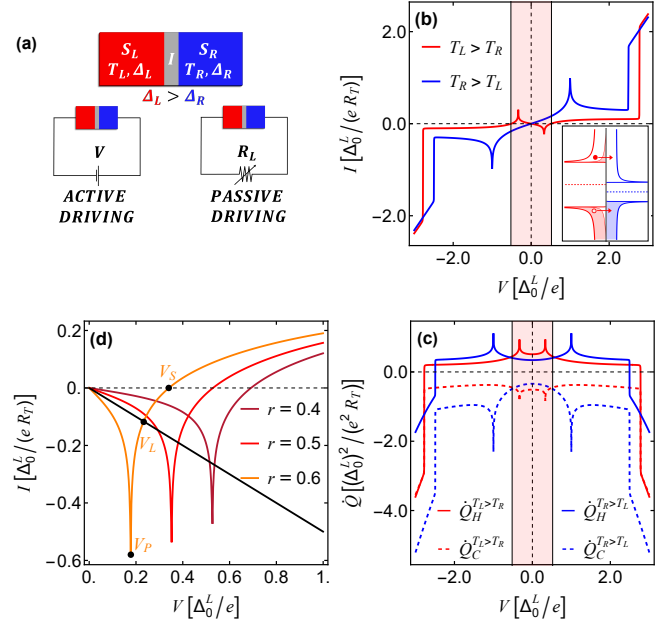


FIG. 1: (a) Scheme of the heat-rectifier coupled to a voltage source (left) and to an external resistor (right) (b)  $I - V$  with  $r = 0.7$  for  $T_L = 0.6T_c^L$  and  $T_R = 0.01T_c^L$  (red), and for the opposite thermal bias  $T_L = 0.01T_c^L$  and  $T_R = 0.6T_c^L$  (blue).  $T_c^L$  is the critical temperature of the bigger gap electrode. The thermoelectric region is reported in pink, while the inset depicts this effect in the energy band diagram. (c)  $\dot{Q} - V$  characteristic, the same parameters as the previous image.  $\dot{Q}_H$  refers to the heat current flowing out from the hot electrode, while  $\dot{Q}_C$  denotes the heat coming to the cold island. The lines' color refers to opposite thermal gradients. (d) Intersection with the load line (black) for  $R_L = 2R_T$  in the thermoelectric regime. Parameters are  $r = 0.4$  (orange),  $r = 0.5$  (red), and  $r = 0.6$  (brown) at fixed  $T_L = 0.8T_c^L$ .

this framework, the quasiparticle transport of heat and charge flowing out the electrode  $\alpha$ , with  $\bar{\alpha}$  labeling the opposite electrode, is described by the following equation<sup>35–37</sup>:

$$\begin{aligned} \begin{pmatrix} \dot{Q}_\alpha \\ I_\alpha \end{pmatrix} &= \frac{1}{e^2 R_T} \int_{-\infty}^{\infty} \begin{pmatrix} E_\alpha \\ -e \end{pmatrix} N_\alpha(E_\alpha, T_\alpha) N_{\bar{\alpha}}(E_{\bar{\alpha}}, T_{\bar{\alpha}}) \\ &\quad \times [f_\alpha(E_\alpha, T_\alpha) - f_{\bar{\alpha}}(E_{\bar{\alpha}}, T_{\bar{\alpha}})] dE. \end{aligned} \quad (1)$$

Here,  $R_T$  denotes the normal state resistance of the junction, and  $N_\alpha(E_\alpha, T_\alpha) = \text{Re} \left[ \frac{E+i\Gamma}{\sqrt{(E+i\Gamma)^2 - \Delta_\alpha(T_\alpha)^2}} \right]$  the normalized smeared BCS quasiparticles Density of States (DOS), with the Dynes parameter  $\Gamma$  effectively accounting for inelastic scattering processes. The electron-hole symmetry in the superconducting DOS, namely  $N_\alpha(E_\alpha, T_\alpha) = N_\alpha(-E_\alpha, T_\alpha)$ , results in symmetric relationships for heat and charge current as functions of the applied voltage, leading to the even symmetry  $\dot{Q}(V, T_L, T_R) = \dot{Q}(-V, T_L, T_R)$  and the reciprocity  $I(V, T_L, T_R) = -I(-V, T_L, T_R)$ , where  $Q(V, T_L, T_R) = Q_R(V, T_L, T_R)$  and  $I(V, T_L, T_R) = I_R(V, T_L, T_R)$ .

When the system is thermoelectric, it exhibits a negative conductance,  $G(V, T_L, T_R) = I(V, T_L, T_R)/V$ , which results in a positive thermoelectric power  $\dot{W} = -IV > 0$ . Due to the electron-hole symmetry, within the linear response regime it is impossible to achieve this condition, as indicated by the current reciprocity<sup>38</sup>. Nonetheless, this becomes feasible in systems operating in a non-linear temperature regime,  $T_L - T_R \gtrsim \Delta T_{min}(r)$ , and characterized by an energy gap ratio  $r = \Delta_R^0/\Delta_L^0 < 1$ . This situation is illustrated in Fig. 1(b), in which we emphasize that the desired bipolar thermoelectric behavior ( $IV < 0$ ) requires heating the higher gap superconducting lead. Specifically, in the subgap region, both the  $IV$  characteristics of the system exhibit a peak at the matching point, which arises from the alignment of BCS singularities at  $V_P = \pm|\Delta_L(T_L) - \Delta_R(T_R)|/e$ . While under normal dissipative regime  $I(V_P, T_C, T_H)V_P > 0$ , in the thermoelectric one  $I(V_P, T_H, T_C)V_P < 0$ , represented by the pink area for the red curve.

In the active driving configuration, the exam of the heat transport in both scenarios reveals interesting dynamics in the sub-gap regime  $eV \lesssim \Delta_L + \Delta_R$ , as we show in Fig. 1(c). When the small gap electrode serves as the hot electrode (blue curves), the heat extracted from it (solid line) is lower than that received by the colder electrode (dashed line). This discrepancy is due to the power injected in the junction by the external voltage source, following from the first law of thermodynamics which requires  $\dot{Q}_R + \dot{Q}_L + IV = 0$ . Conversely, in the opposite thermal bias, the system may generate bipolar thermoelectricity. In this condition, the power generated in the external circuit ( $IV < 0$ ) is obtained at the expense of the heat flowing out from the hotter side (solid) while, correspondingly, the heat in the colder one is reduced (dashed). This is the behaviour of a typical thermoelectric device which operates as a thermodynamical engine producing power dissipated in the external circuit. This peculiar thermoelectricity only operates in a range of voltages  $|V| \leq V_S$  (pink area in the figures), where  $V_S$  is the Seebeck voltage marking the open-circuit condition  $I(V_S, T_L, T_R) = 0$ . Increasing further the applied voltage leads the system to recover the dissipative behavior and the Joule heating warms both leads, resulting in all heat fluxes turning negative.

Moreover, the inherent asymmetry between the superconducting gaps naturally facilitates the flow of heat from the electrode with the larger gap to the one with the smaller gap. However, we anticipate that the generation of thermoelectric power, which may occur when the side with the higher gap is

heated, further amplifies the non-reciprocal nature of the heat flow. To harness the full potential of our system, we focus on the circuit configuration with passive driving displayed on the right side of Fig. 1(a), where the junction is only closed on a load resistor  $R_L$ . In this arrangement, the current and the bias are determined by solving:

$$I(V_L, T_L, T_R) + \frac{V_L}{R_L} = 0. \quad (2)$$

This equation yields a non-zero  $V_L \neq 0$  solution exclusively in thermoelectric conditions ( $IV_L < 0$ ). Specifically, when the load line intersects the I-V curve within this region, the system can exhibit an odd number of distinct solutions (usually three metastable, referring to solutions with positive differential conductance<sup>28</sup>). In particular, the particle-hole symmetric point  $V = 0$  is metastable<sup>26,28,33,34</sup>. However, by applying a bias current  $I_B$ , it becomes possible to select another thermoelectric metastable solution characterized by  $V = \pm V_L$ , with the sign determined by the polarity of  $I_B$ . Importantly, once this state is activated by  $I_B$ , the system maintains this solution even after  $I_B$  is reset to zero<sup>28</sup> due to the spontaneous particle-hole symmetry mechanism behind the bipolar thermoelectricity<sup>26</sup>. For a specific resistor, the value of  $|V_L|$  lies in the range  $|V_P| \leq |V_L| \leq |V_S|$ , as illustrated in Fig. 1(d) for different gap ratios  $r$ , and by the applied thermal bias. Optimal thermoelectric performance occurs near the matching peak  $V_P$ , but it decreases as it approaches the Seebeck voltage  $V_S$ . In the passive driving configuration, the operating points in the thermoelectric phase determine the heat current rectification performance of our system. This allows us to characterize it as a passive thermal diode, where we refer to the stationary condition.

To quantify this non-reciprocity we introduce the heat-transport rectification coefficient  $\mathcal{R}$  as follows:

$$\mathcal{R}(V_L) = \frac{\dot{Q}^+(V_L) - \dot{Q}^-(0)}{\dot{Q}^-(0)} \times 100, \quad (3)$$

where we define  $\dot{Q}^+(V_L) = \dot{Q}_R(T_L = T_H, T_R = T_C, V_L)$  as the magnitude of the heat current when the electrode with the larger gap is heated and  $\dot{Q}^-(0) = \dot{Q}_R(T_L = T_C, T_R = T_H, V = 0)$  when the direction of the thermal bias is reversed. We stress that only when the system is thermoelectric a non-null stable solution  $V_L \neq 0$  of Eq. 2 is possible.

Firstly, we start to compare the rectification at  $V_L = 0$ , assuming that the SIS' junction remains trapped in the non-thermoelectric metastable phase. This case, which has been also considered before<sup>24,39</sup> and it could happen when the Josephson coupling is sufficiently strong shortening the junction that remains trapped at  $V_L = 0$  not developing any thermoelectricity<sup>33,34</sup>. In Fig. 2(a) we show the evolution of the rectification by gap asymmetry  $r$  and hot-lead temperature  $T_H$ , assuming to fix the cold temperature at  $T_C = 0.01T_c^L$ . We report rectification values up to approximately  $\mathcal{R}_{max} \approx 260\%$ , albeit within a constrained parameter space of  $T_H$  and  $r$ . In contrast, when the phenomenon of thermoelectricity is present it markedly enhances this effect and broadens the applicable conditions, as highlighted in Figure 2(b) for  $V_L = V_P$ . Indeed,

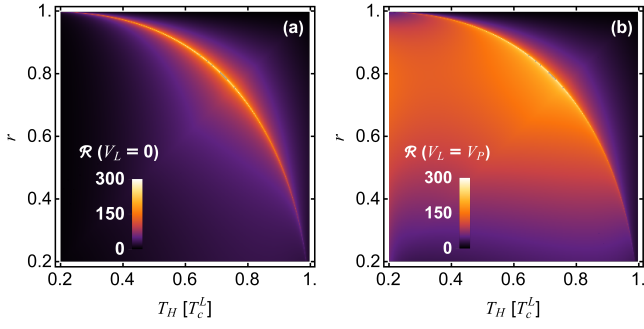


FIG. 2: Rectification efficiency  $\mathcal{R}$  vs  $(T_H, r)$  at  $V_L = 0$  in (a) and at  $V_L = V_P$  in (b). In both cases we set  $T_C = 0.01T_c^L$ .

at this operating point, the thermoelectricity is maximal as well as the heat extraction from the hot electrode. Clearly, to adopt this operational point one necessarily needs to optimize the value of load resistance. Therefore, it is worth exploring how the effect remains evident when we consider a fixed load resistor, a case that resembles the expected operational use of the device. This persistence is demonstrated in Fig. 3(a) (Fig. 3(b)) where we consider a fixed resistor  $R_L = 0.5R_T$  ( $R_L = R_T$ ), indicating that substantial heat rectification performance is achievable even without a precise tuning of the load to the parameter variation. In Fig. 3(c) we report, as a function of  $T_H$  for fixed  $r = 0.8$ , the comparison between the two previous cases and the case of a shortened circuit  $R_L = 0$ , i.e.  $V_L = 0$ . We see that the large values of heat rectification are widened with respect to the resonant value, enhancing its resilience to thermal fluctuations. Specifically, as we can see in Fig. 3(d), choosing a higher  $R_L$  results in a lower slope of the load line. This increases the range over which non-null thermoelectric solutions of Eq. 2 can exist.

In addition, the incorporation of a resistor means that a specific amount of power,  $W = I_L V_L$ , is delivered by the junction to this external component, where it is dissipated as Joule heating. This feature introduces the potential to create a purely electronic heat pipe to be used in cryogenic electronics. Indeed, the Joule heating is concentrated in the resistor, which can be placed at a large distance from the junction and thus in principle allowing even to bring the heat outside the local cryogenic environment. This enables an efficient thermal management since the heat dissipated in the cold lead is now less than the heat extracted by the hot lead, as ruled by the first law of thermodynamics. To quantify the heat piping efficiency in this scenario we introduce a figure of merit,  $\mathcal{P}$ , defined by the equation:

$$\mathcal{P} = \frac{W}{\dot{Q}_R}, \quad (4)$$

Where  $W$  refers to the thermoelectric power that can be transported out of the low-temperature environment via the electronic heat pipe while  $\dot{Q}_R$  is the heat arriving at the cold terminal. In this way we can reduce the necessary cooling power at the lowest temperature stage of the setup.

Initially, we set the resistor to  $R = R_T$  in Fig. 4(a), demonstrat-

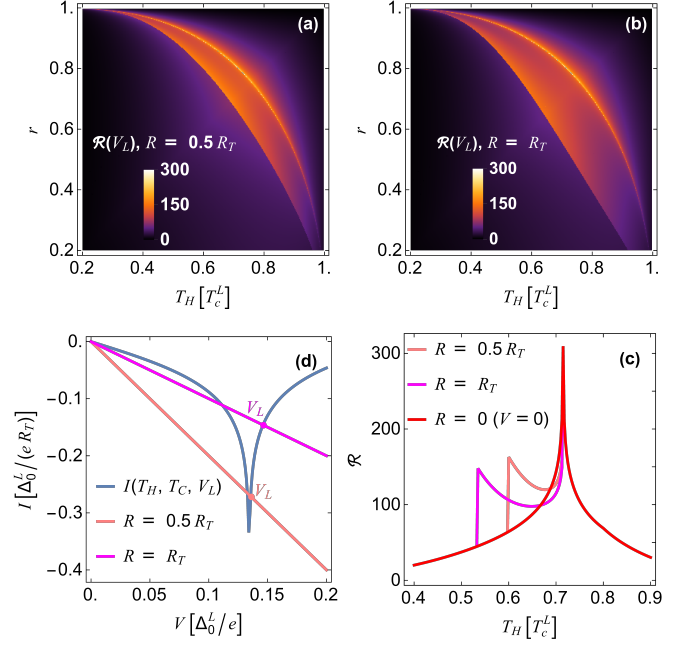


FIG. 3: (a-b) Rectification efficiency  $\mathcal{R}$  vs  $(T_H, r)$  at  $V = V_L$  for  $R = 0.5R_T$  and  $R = R_T$ . In both cases, we set  $T_C = 0.01T_c^L$ . (c)  $\mathcal{R}$  vs  $T_H$  for  $R = 0.5R_T$ ,  $R = R_T$  and  $R = 0$  at  $r = 0.8$ . (d) Intersection between the load lines and  $I(V, T_H, T_C)$  for  $T_H = 0.8T_c^L$ ,  $T_C = 0.01T_c^L$  and  $r = 0.8$ .

ing that up to 20% of the thermal flux meant for the cold electrode can be redirected towards the load. Specifically, In Fig. 4(b) we see how the heat fluxes and the thermoelectric power change with  $T_H$  for a given value of gap ratio  $r$ . Intriguingly we note that thermoelectric contribution plays an important role when the temperature deviates from the optimal peak values. In a subsequent analysis, shown in Fig. 4(c), we kept the gap ratio constant while modifying resistance values. This approach revealed that increasing resistance substantially improves the system's efficiency in redirecting a part of the thermal flow to the resistor, with  $\mathcal{P}$  approaching roughly 65% in high-resistance configurations. However, this enhancement is balanced by the decrease in the amount of heat effectively redirected (thermoelectric power  $W$ ), greater for load in the order of the tunnelling resistance, as demonstrated in Fig. 4(d).

Finally, we can discuss the potential experimental implementation of this system. We aim to establish quasi-equilibrium conditions, where both the quasi-particle temperature  $T_{QP}$  and the phonon bath temperature  $T_{Ph}$  are well-defined but can be different. This is feasible in a superconductor, where the quasiparticle-phonon heat flux is exponentially damped below the critical temperature<sup>40</sup>. Specifically, a suitable candidate to develop these devices is aluminum, whose excellent quality of Aluminum-oxide junctions allows the fabrication of SQUID architectures that enable the suppression of the Josephson contribution through the application of an external magnetic field. To achieve a device with gap ratio  $r \neq 1$ , we can exploit the inverse proximity effect, combining Al with

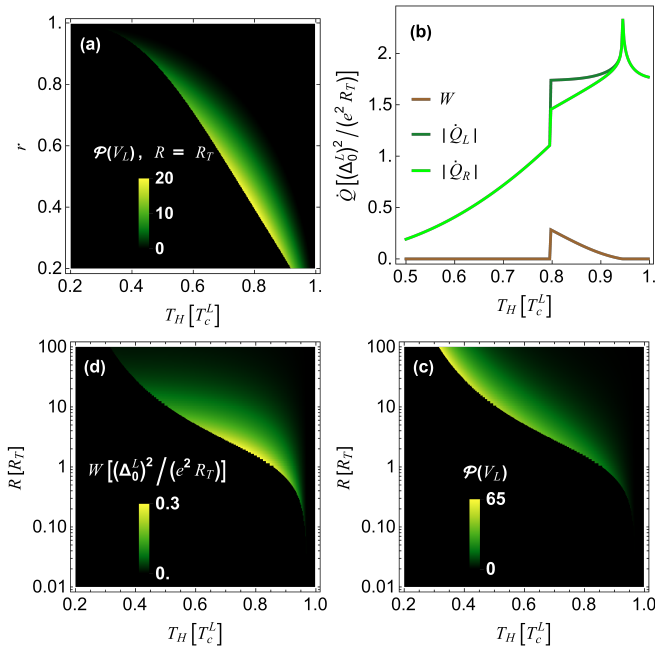


FIG. 4: (a)  $\mathcal{P}$  vs  $(T_H, r)$  for  $R = R_T$ . (b) comparison between the heat current  $\dot{Q}_L$  flowing out from the L electrode, the one  $\dot{Q}_R$  coming to the right and power  $W$  dissipated on the resistor. (c)  $\mathcal{P}$  for different values of the resistor  $R_L$  and  $T_H$ , calculated for  $r = 0.4$ . (d) map of the power  $W$  dissipated on the resistor in the same conditions of (c).

other superconductors or normal metals in bilayers to reduce the gap of one of the electrodes<sup>29</sup>. For example, in the experimental evidence discussed in Ref. 28, the choice fell on Al/Cu bilayer, resulting in a ratio  $r \sim 0.35$ .

In conclusion, our research delved into the thermal transport dynamics of asymmetric  $SIS'$  Josephson junctions, emphasizing the role of bipolar thermoelectricity within these systems. We successfully demonstrated how this particular regime enhances both the thermal bias and the gap ratio range over which the system acts as a good thermal diode with respect to the non-thermoelectric phase of  $SIS'$ . Moreover, we revealed the potential of exploiting a load resistor to dissipate away the heat from the electrode with the larger energy gap. Finally, the harvested energy can be redirected in a NIS cooling device to further increase the heat-removing capabilities of the system. This finding is especially compelling from an energy management perspective, introducing an innovative twist to conventional electrical heat piping strategies that further enhance the constrained cooling capabilities, particularly crucial at the ultra-low temperatures experienced by cold fingers. This advancement could be pivotal in improving heat control and energy harvesting within superconducting quantum technologies, marking a step forward in optimizing their operational efficiency.

## ACKNOWLEDGMENTS

We acknowledge the EU's Horizon 2020 Research and Innovation Framework Programme under Grant No. 964398 (SUPERGATE), No. 101057977 (SPECTRUM), and the PNRR MUR project PE0000023-NQSTI for partial financial support. A.B. acknowledges also the MUR-PRIN2022 Project NETheQS (Grant No. 2022B9P8LN), the Royal Society through the International Exchanges between the UK and Italy (Grants No. IEC R2 192166) and CNR project QTHERMONANO.

## DATA AVAILABILITY

The data that support the findings of this study are available from the corresponding author upon reasonable request.

## AUTHOR DECLARATIONS

The authors have no conflicts to disclose.

- <sup>1</sup>F. Giazotto and J. P. Pekola, "Josephson tunnel junction controlled by quasiparticle injection," *J. Appl. Phys.* **97** (2005).
- <sup>2</sup>F. Giazotto, T. T. Heikkilä, A. Luukanen, A. M. Savin, and J. P. Pekola, "Opportunities for mesoscopies in thermometry and refrigeration: Physics and applications," *Rev. Mod. Phys.* **78**, 217 (2006).
- <sup>3</sup>J. T. Muhonen, M. Meschke, and J. P. Pekola, "Micrometre-scale refrigerators," *Rep. Prog. Phys.* **75**, 046501 (2012).
- <sup>4</sup>A. Fornieri, M. J. Martínez-Pérez, and F. Giazotto, "A normal metal tunnel-junction heat diode," *Appl. Phys. Lett.* **104** (2014).
- <sup>5</sup>J. P. Pekola and B. Karimi, "Colloquium: Quantum heat transport in condensed matter systems," *Rev. Mod. Phys.* **93**, 041001 (2021).
- <sup>6</sup>A. Braggio, M. Carrega, B. Sothmann, and R. Sánchez, "Nonlocal thermoelectric detection of interaction and correlations in edge states," *Phys. Rev. Res.* **6**, L012049 (2024).
- <sup>7</sup>M. Nahum, T. M. Eiles, and J. M. Martinis, "Electronic microrefrigerator based on a normal-insulator-superconductor tunnel junction," *Appl. Phys. Lett.* **65**, 3123–3125 (1994).
- <sup>8</sup>G. Marchegiani, P. Virtanen, and F. Giazotto, "On-chip cooling by heating with superconducting tunnel junctions," *EPL* **124**, 48005 (2018).
- <sup>9</sup>B. Sothmann, R. Sánchez, and A. N. Jordan, "Thermoelectric energy harvesting with quantum dots," *Nanotech.* **26**, 032001 (2014).
- <sup>10</sup>H. Thierschmann, R. Sánchez, B. Sothmann, F. Arnold, C. Heyn, W. Hansen, H. Buhmann, and L. W. Molenkamp, "Three-terminal energy harvester with coupled quantum dots," *Nat. Nanotech.* **10**, 854–858 (2015).
- <sup>11</sup>M. Martín-González, O. Caballero-Calero, and P. Díaz-Chao, "Nano-engineering thermoelectrics for 21st century: Energy harvesting and other trends in the field," *Renew. Sustain. Energy Rev.* **24**, 288–305 (2013).
- <sup>12</sup>G. Jaliel, R. Puddy, R. Sánchez, A. Jordan, B. Sothmann, I. Farrer, J. Griffiths, D. Ritchie, and C. Smith, "Experimental realization of a quantum dot energy harvester," *Phys. Rev. Lett.* **123**, 117701 (2019).
- <sup>13</sup>C. Enss, *Cryogenic particle detection*, Vol. 99 (2005).
- <sup>14</sup>F. Paolucci, G. Germanese, A. Braggio, and F. Giazotto, "A highly sensitive broadband superconducting thermoelectric single-photon detector," *Appl. Phys. Lett.* **122** (2023).
- <sup>15</sup>R. Sánchez, H. Thierschmann, and L. W. Molenkamp, "Single-electron thermal devices coupled to a mesoscopic gate," *New J. Phys.* **19**, 113040 (2017).
- <sup>16</sup>Y. Zhang and S. Su, "Thermal rectification and negative differential thermal conductance based on a parallel-coupled double quantum-dot," *Phys. A: Stat. Mech. Appl.* **584**, 126347 (2021).
- <sup>17</sup>W. Kobayashi, "Thermal-rectification coefficients in solid-state thermal rectifiers," *Phys. Rev. E* **102**, 032142 (2020).



- <sup>18</sup>C. W. Chang, D. Okawa, A. Majumdar, and A. Zettl, “Solid-state thermal rectifier,” *Science* **314**, 1121–1124 (2006).
- <sup>19</sup>F. K. Malik and K. Fobelets, “A review of thermal rectification in solid-state devices,” *J. Semicond.* **43**, 103101 (2022).
- <sup>20</sup>H. Wang, S. Hu, K. Takahashi, X. Zhang, H. Takamatsu, and J. Chen, “Experimental study of thermal rectification in suspended monolayer graphene,” *Nat. Comm.* **8**, 15843 (2017).
- <sup>21</sup>B. Bhandari, P. A. Erdman, R. Fazio, E. Paladino, and F. Taddei, “Thermal rectification through a nonlinear quantum resonator,” *Phys. Rev. B* **103**, 155434 (2021).
- <sup>22</sup>A. Iorio, E. Strambini, G. Haack, M. Campisi, and F. Giazotto, “Photonic heat rectification in a system of coupled qubits,” *Phys. Rev. Appl.* **15**, 054050 (2021).
- <sup>23</sup>G. Marchegiani, A. Braggio, and F. Giazotto, “Highly efficient phase-tunable photonic thermal diode,” *Applied Physics Letters* **118** (2021).
- <sup>24</sup>M. Martínez-Pérez and F. Giazotto, “Efficient phase-tunable josephson thermal rectifier,” *Appl. Phys. Lett.* **102** (2013).
- <sup>25</sup>F. Giazotto and F. Bergeret, “Very large thermal rectification in ferromagnetic insulator-based superconducting tunnel junctions,” *Appl. Phys. Lett.* **116** (2020).
- <sup>26</sup>G. Marchegiani, A. Braggio, and F. Giazotto, “Nonlinear thermoelectricity with electron-hole symmetric systems,” *Phys. Rev. Lett.* **124**, 106801 (2020).
- <sup>27</sup>G. Marchegiani, A. Braggio, and F. Giazotto, “Superconducting nonlinear thermoelectric heat engine,” *Phys. Rev. B* **101**, 214509 (2020).
- <sup>28</sup>G. Germanese, F. Paolucci, G. Marchegiani, A. Braggio, and F. Giazotto, “Bipolar thermoelectric josephson engine,” *Nat. Nanotechnol.* **17**, 1084–1090 (2022).
- <sup>29</sup>A. Hijano, F. Bergeret, F. Giazotto, and A. Braggio, “Bipolar thermoelectricity in  $s/i/ns$  and  $s/i/sn$  superconducting tunnel junctions,” *Appl. Phys. Lett.* **122** (2023).
- <sup>30</sup>S. Battisti, G. De Simoni, L. Chiroli, A. Braggio, and F. Giazotto, “Bipolar thermoelectric superconducting single-electron transistor,” *Phys. Rev. Res.* **6**, L012022 (2024).
- <sup>31</sup>C. Guarcello, R. Citro, F. Giazotto, and A. Braggio, “Bipolar thermoelectrical squipt (btsquipt),” *Appl. Phys. Lett.* **123** (2023).
- <sup>32</sup>L. Bernazzani, G. Marchegiani, F. Giazotto, S. Roddaro, and A. Braggio, “Bipolar thermoelectricity in bilayer-graphene–superconductor tunnel junctions,” *Phys. Rev. Applied* **19**, 044017 (2023).
- <sup>33</sup>G. Marchegiani, A. Braggio, and F. Giazotto, “Phase-tunable thermoelectricity in a josephson junction,” *Phys. Rev. Research* **2**, 043091 (2020).
- <sup>34</sup>G. Germanese, F. Paolucci, G. Marchegiani, A. Braggio, and F. Giazotto, “Phase control of bipolar thermoelectricity in josephson tunnel junctions,” *Phys. Rev. Applied* **19**, 014074 (2023).
- <sup>35</sup>M. Tinkham, *Introduction to superconductivity* (Courier Corporation, 2004).
- <sup>36</sup>P.-G. De Gennes, *Superconductivity of metals and alloys* (CRC press, 2018).
- <sup>37</sup>T. O. Wehling, A. M. Black-Schaffer, and A. V. Balatsky, “Dirac materials,” *Adv. Phys.* **63**, 1–76 (2014).
- <sup>38</sup>G. Benenti, G. Casati, K. Saito, and R. S. Whitney, “Fundamental aspects of steady-state conversion of heat to work at the nanoscale,” *Phys. Rep.* **694**, 1–124 (2017).
- <sup>39</sup>A. Fornieri, M. J. Martínez-Pérez, and F. Giazotto, “Electronic heat current rectification in hybrid superconducting devices,” *AIP Adv.* **5** (2015).
- <sup>40</sup>A. Timofeev, C. P. Garcia, N. Kopnin, A. Savin, M. Meschke, F. Giazotto, and J. Pekola, “Recombination-limited energy relaxation in a bardeen-cooper-schrieffer superconductor,” *Phys. Rev. Lett.* **102**, 017003 (2009).
- <sup>41</sup>A. Fornieri and F. Giazotto, “Towards phase-coherent caloritronics in superconducting circuits,” *Nat. Nanotech.* **12**, 944–952 (2017).
- <sup>42</sup>M. J. Martínez-Pérez, A. Fornieri, and F. Giazotto, “Rectification of electronic heat current by a hybrid thermal diode,” *Nat. Nanotech.* **10**, 303–307 (2015).